Pergamon

Bioorganic & Medicinal Chemistry, Vol. 5, No. 10, pp 1943–1957, 1997

PII: S0968-0896(97)00132-6
0968-0896/97 $17.00 + 0.00

Structure of Kainic Acid Totally Elucidated by NMR and Molecular Modelling

Nathalie Todeschi,[a] Josyane Gharbi-Benarous[a,b] and Jean-Pierre Girault[a,*]

[a]*Université René Descartes-Paris V, Laboratoire de Chimie et Biochimie Pharmacologiques et Toxicologiques (URA 400 CNRS), 45 rue des Saint-Pères, 75270 Paris Cedex 06, France*

[b]*Université Denis Diderot-Paris VII, UFR Chimie, 2 Place Jussieu, F-75251 Paris Cedex 05, France*

Abstract—One class of glutamate receptors is characterized by the binding of the neuroexcitant and toxin kainic acid (KA), which contains an embedded L-glutamate moiety in a partially restricted (about the 2,3-bond) conformation. While there are a number of compounds that exhibit high specificity and selectivity at the ionotropic *N*-methyl-D-aspartate receptor, there has been a lack of selective and high-affinity ligands for the ionotropic KA subclass of excitatory amino acid receptors. This substance has received some attention recently being the least understood of the ionotropic type of glutamate receptor. The spatial orientation of the perceived functional groups of KA has been elucidated by a conformational analysis of an aqueous solution of KA using a combination of nuclear magnetic resonance (NMR) experimental results, mechanics and dynamics calculations, and theoretical simulation of NMR spectra. The weak pH-dependent effects on overall conformation and the structure of the principal '**E**-*envelope*' KA conformer are established in aqueous solution. This study clearly shows the structural 'down' position of the double bond and the preferred 'g^--c' conformation of the C(3) carboxymethyl side-chain. The complex structure of this compound is thus definitively resolved. The conformation of the *envelope* ring such as C(3) carboxymethyl and C(4)-isopropenyl groups may strongly influence the potencies of KA interactions with the KA receptor. © 1997 Elsevier Science Ltd.

Introduction

L-Glutamate, a major excitatory neurotransmitter in the central nervous system (CNS),[1,2] plays an important role in neuronal plasticity and neurotoxicity. However, excessive release of glutamic acid can result in neuronal death, a phenomenon that has been termed excitotoxicity.[3–6] Converging lines of evidence indicate that excitotoxic cell death sustantially contributes to the pathophysiology of both acute (stroke) and chronic (Alzheimer's) neurodegenerative disorders in the CNS.[7] As with other neurotransmitter receptors, glutamate receptors have been classified into two disctinct groups termed ionotropic receptors and metabotropic receptors (mGluRs). The ionotropic receptors[8,9] comprise integral cation-specific channel complexes and are further subdivided into the receptors for *N*-methyl-D-aspartate (NMDA) and the non-NMDA receptors for kainic acid (KA) and α-amino-3-hydroxy-5-methyl-4-isoxazolepropionate (AMPA) according to their selective actions as agonists.[1,2] The mGluRs are coupled to intracellular second-messenger systems.[10–12]

It is reasonable to assume that L-glutamate has different conformations (Fig. 1a) resulting from the rotation around the C(2)–C(3) (χ_1) and C(3)–C(4) (χ_2) bonds and thus is capable of fitting the different types of receptors.[13]

The KA subclass of excitatory amino acid (EAA) receptors was originally identified and characterized by its selective interaction with a marine natural product, α-KA, first isolated from the seaweed *Digenea simplex*. KA has been used as a successful probe for the analysis of the physiological functions of excitatory amino acids since they have potent activity in the vertebrate and invertebrate glutamatergic system.[14–16] The potent neuroexcitatory activity of KA possibly depends on the restricted conformation of the glutamate skeleton involved as a constitutional structure. On the other hand, recent studies demonstrate the high sensitivity of the isopropylene side-chain to some changes.[17–20] Replacement of the isopropenyl group by

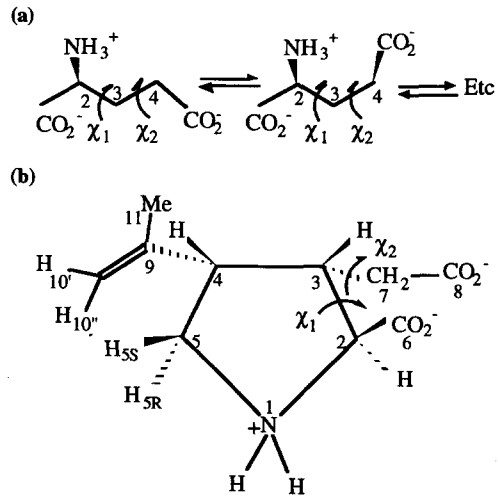

Figure 1. (a) Conformers of L-glutamate; (b) structure of kainic acid in aqueous solution at pH 7 (isomers α-S represented).

aromatic fragments shows increments of activities and removal of the double bond from the C(4) position of the proline ring shows reduction. Acromelic acid shows potent activities, while dihydrokainic acid shows little activity and is no longer a kainate agonist but an uptake inhibitor.[21] In the same way, it is noteworthy that the activity of the dihydro-derivative of CPG-IV [2-(2-carboxy-4-methylenecyclopentyl)glycine], a potent agonist of kainate receptors[22] was much less than CPG-IV. The *exo* methylene group of CPG-IV appeared to be essential to activate kainate receptors as the same way as the C–C double bond of KA is required for its activity.

KA (Fig. 1b) contains an embedded L-glutamate moiety [C(6)–C(2)–C(3)–C(7)–C(8)], exhibiting a partially restricted rotation around the C(2)–C(3) (χ_1) and C(3)–C(7) (χ_2) bonds. KA represents a conformationally restricted analogue, but it retains some flexibility and therefore multiple conformers are likely to be populated in solution.

The conformational analysis of this compound in solution was difficult to elucidate because of its structural characteristics constituted by three flexible moieties (Fig. 2):

(1) A five-membered ring, pyrrolidine: the strain in the molecule is partly relieved by puckered conformations. Two flexible forms exist, namely *envelope* **E** and *half-chair* or twist **T** conformers (Fig. 2b, c). In these conformers, the following types of exocyclic bonds have been recognized: equatorial (e), axial (a) and isoclinal (i) bonds. The two conformers **E** and **T** are extremes of symmetry in the pseudorotational circuit of the five-membered ring (Fig. 2a). The envelope and the half-chair forms interconvert by the pseudorotation process which is almost of constant strain. An accurate description of the ring will be given by the use of the $^3J_{H,H}$ and $^3J_{H,C}$ coupling constants.

(2) A carboxymethyl group at the C(3) position leads to a fluctuating angle χ_2: three 'staggered' rotamers (*gauche* and *anti*) result from the rotation around the torsion angle [C(3)–C(7)] (Fig. 3).

(3) A 4-isopropenyl group: the free rotation around the C(4)–C(9) bond corresponds to the two positions of the

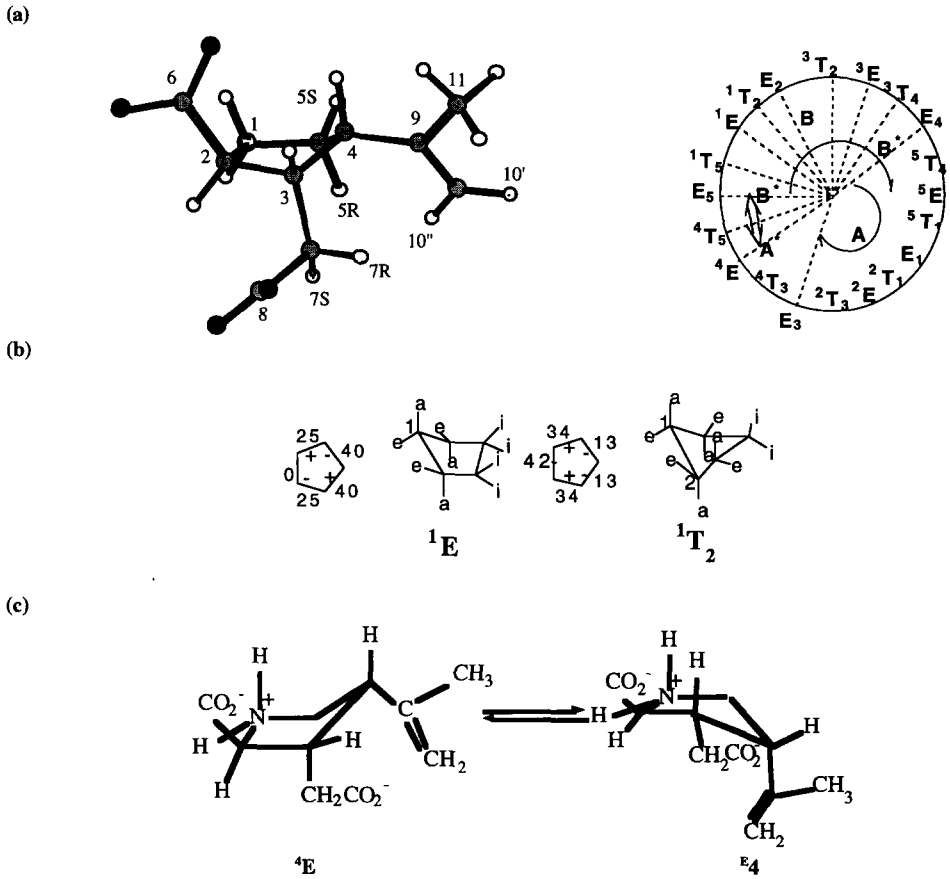

Figure 2. (a) Structure of kainic acid (KA) at neutral pH: *envelope* conformation ^{4}**E** for KA at pH 7. Pseudorotational pathway of the five-membered ring. Each external point of dotted radials in the circle represents a specific E form or T conformation generated by molecular modelling. (b) Considered conformations for cyclopentane. The forms, *envelope* **E** and *half-chair* or *twist* **T** are represented in perspective drawing, as well as in the conventional formula indicating the approximate value of the torsion angles and their sign and with the following types of exocyclic bonds: *equatorial (e), axial (a)*, and the so-called *isoclinal (i)* bonds. The former has four carbons in the same plane. In contrast, the half-chair has three coplanar carbon atoms, one above and one below (^{1}**T**$_2$). (c) Conformational equilibrium between the structure ^{4}**E** and **E**$_4$.

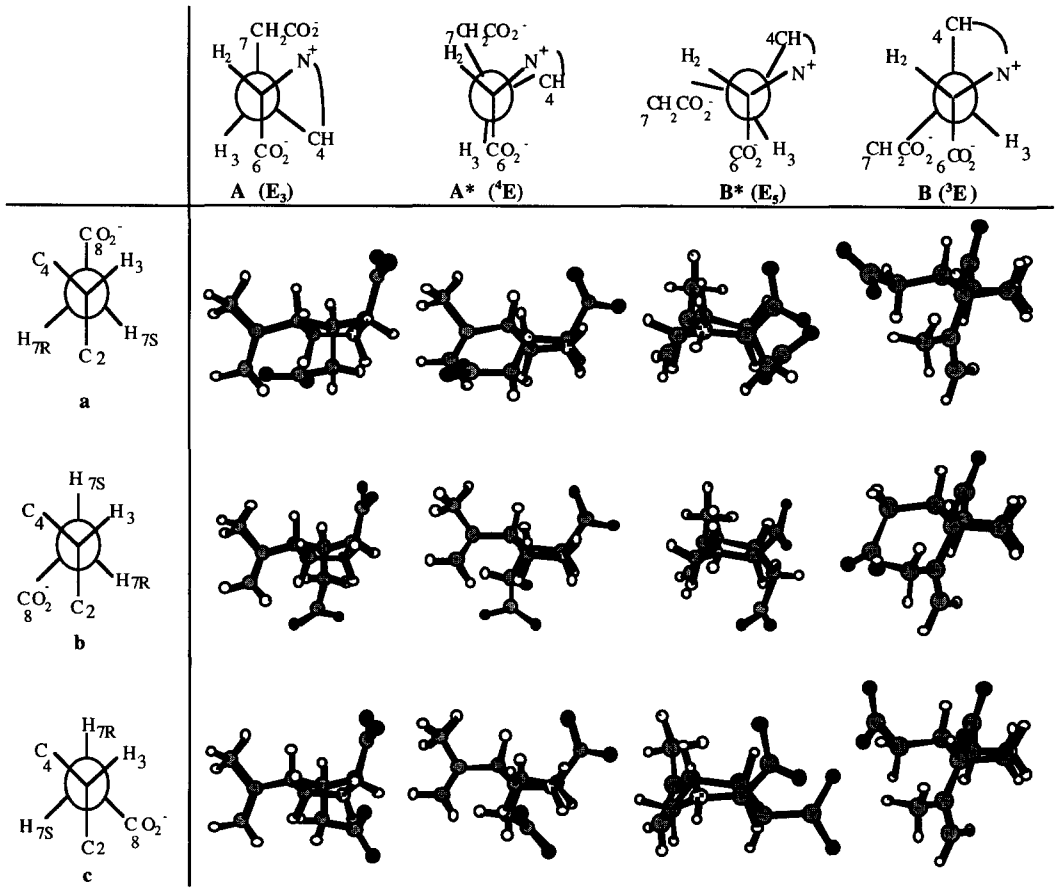

Figure 3. The rotamers 'A, A*, B*, and B' relative to the torsion angle χ_1 corresponding to the 10 *envelopes* of kainic acid. Newman projections for these rotamers and 'a, b, c' relative to the χ_2 one.

double bond relative to H(4), 'eclipsed' (or 'up') and '*anti*' (or 'down') (Fig. 4).

Considering the interaction between kainate and its receptor, the three functional groups, namely the two carboxyl and one amino groups of the glutamic acid moiety, in addition to the C(4)-substituent (isopropenyl group) should be adequately arranged to favorably fit into the receptor. The pyrrolidine ring should play a role in arranging the spatial position of these functional groups in the kainoid molecules.[17,23–26] Despite numerous efforts reported by Shimamoto and Ohfune,[27] the kainate conformation has not yet been elucidated (for example, the C(3) acetic acid group, the five-membered ring or the orientation of the isopropenyl group), thus this study allows us to shed light on the resulting conformation of KA in aqueous solution.

The conformation binding to the receptor will be either the major conformation populated in solution or an high-energy conformation. It seems difficult to reach a particular high negative ΔG for favourable binding to

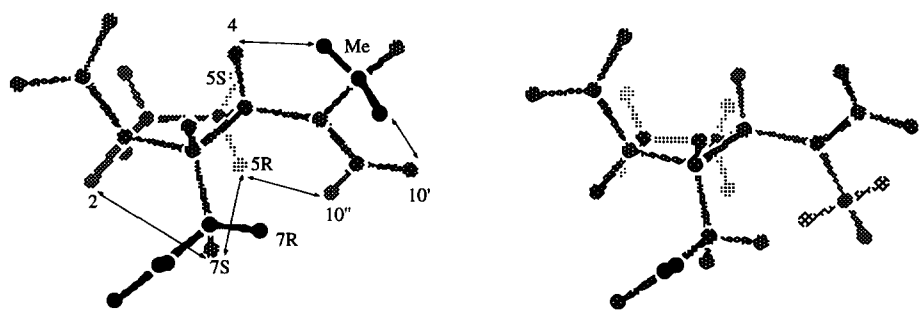

Figure 4. The ^{1}H NOE connectivities are represented for the structure '**c**' (^{4}**E**).

the KA receptor if the different groups potentially active in the binding site (α-CO_2^-, α-NH_3^+ and γ-CO_2^-) do not present beforehand a particular spatial topology. Thus NMR parameters reflect the virtual conformational solution and at the same time the structural information of the different conformations generated by molecular dynamics (MD) are of great benefit in predicting the conformations in solution. In addition, the MD calculations may indicate a range of conformers of higher energy which may potentially be accessible to the molecule.

Results and Discussion

In order to gain some insight into its possible conformations, we have undertaken a conformational analysis of KA by 1-D ^1H and ^{13}C NMR, 2-D NMR techniques (^1H–^1H COSY, NOESY and 2-D J-δ selective INEPT) and molecular modelling. As MD calculations deal with the energy and geometry of individual conformations, whereas NMR data are averaged over different conformations, this study serves to correlate the two methods. We have extended the NMR and the MD study in water at different pH values, so as not to neglect protonation sites which will induce particular conformations. The final structures obtained after several molecular mechanics and dynamics calculations (MM and MD) were examined for the overall energetic favorability and compared with the structure derived from the NMR data. The torsion angles of generated structures can be correlated with the corresponding coupling constants by using Karplus-type equations.[28-30] The agreement of the generated structures with the experimental NMR coupling constants is then examined.

Conformational analysis

For L-glutamate, there is a high degree of liberty around the C(2)–C(3) torsion angle χ_1 and the C(3)–C(4) torsion angle χ_2 (Fig. 1). The C(2)–C(3)–C(4) system with two C–C single bonds allows the possibility of *trans* and *gauche* forms and there are a total of $3 \times 3 = 9$ rotamers, all of which are distinct. For L-glutamate, nine 'staggered' conformations result from the combination of the three rotamers 'A, B, C' (rotation about χ_1) with the three rotamers 'a, b, c' (rotation about χ_2). It was of interest to identify which of those conformations (Aa, Ab, Ac, ...) correspond to the embedded L-glutamate structure in KA structure and is able to fit to the KA in all probability.

Rotation around χ_1 [C(2)–C(3) bond]

KA has a much more restricted rotation around the C(2)–C(3) bond than the L-glutamate, but in principle, some of the populations analogous to those of L-glutamate may be populated in KA. The g^--C conformation corresponding to χ_1 [α-CO_2^-–C(2)–C(3)–C(7)] = $-60°$ is inappropriate because of the five-membered ring. The fluctuation of this torsion angle (70–170°) leads to two 'staggered' conformations (t-A and g^+-B) and two 'eclipsed' forms (e-B* and e-A*) favoured by the five-membered ring. These 'eclipsed' forms are characterized by angle values intermediate between gauche g^+-B and antiperiplanar t-A orientations (Fig. 3).

The following four χ_1 [α–CO_2^-–C(2)–C(3)–C(7)] rotamers are observed according to the 10 *envelopes* of the five-membered ring:

t-A (χ_1=150–170°), $\mathbf{E}_1$, $^2\mathbf{E}$, and $\mathbf{E}_3$ *envelopes*.

e-A* (χ_1=130–150°), $^4\mathbf{E}$ *envelope*.

e-B* (χ_1 = 90–120°), $\mathbf{E}_5$ and $^5\mathbf{E}$ *envelopes*.

g^+-B (χ_1 = 70–90°), $^1\mathbf{E}$, $\mathbf{E}_2$, $^3\mathbf{E}$, and $\mathbf{E}_4$ *envelopes*.

Rotation around χ_2 [C(3)–C(7) bond]

As for L-glutamate, there is a high degree of liberty around the χ_2 C(3)–C(7) torsion angle. The C(2)–C(3)–C(7) system with a free single bond allows the possibility of *trans* (t-a) and *gauche* (g^+-b, g^--c) forms (Fig. 3). For each of the previous ten *envelopes* correspond three rotamers (a, b, and c) and thus a total of 30 conformations has to be considered .

Rotation around the double bond

The free rotation around the single bond C(4)–C(9) allows two positions ('up' and 'down') of the double bond (Fig. 4). Sixty conformations are obtained resulting from the combination of the 'A, A*, B*, B' χ_1 rotamers (10 *envelopes*), of the three 'a, b, c' χ_2 rotamers (Fig. 3) and of the two ('up' and 'down') positions of the double bond. As the orientation of the double bond can be resolved before the beginning of the MD study, only 30 conformers will be considered as starting structures for the molecular modelling study.

NMR spectroscopy

Assignments. The assignments were made in D_2O solution at different pH values: 3 (isoelectric), 7 (neutral), and 11 (basic) using 1-D ^1H and ^{13}C (^1H decoupled and DEPT-135)[31] spectra and 2-D heteronuclear (F1 decoupled)[32,33] shift correlations. The results are summarized in Tables 1–5.

From the ^1H NMR spectrum at 500.13 MHz, the starting point was the signal of the H(2) proton, which has a higher resonance frequency than the other protons (because of the adjacent α-CO_2^- and α-NH_3^+ groups). ^{13}C NMR (125.76 MHz) also proved useful. In particular, a one-dimensional selective INEPT experiment based on a selective excitation of the H(2) proton, was useful to differentiate both α- and γ-carboxylate

Table 1. ^1H chemical shifts in D_2O at various pH values (δ_H/[$^2H_4$]TSP error 0.01 ppm) and ^{13}C chemical shifts in D_2O at pH 7 (δ_C/[$^2H_4$]TSP error 0.1 ppm)

	KA					
	pH3		pH11		pH7	
	^1H	^{13}C	^1H	^{13}C	^1H	^{13}C
2	4.14	68.4	3.87	69.2	4.05	68.7
3	3.10	43.4	2.95	45.6	3.03	44.8
4	3.03	48.5	2.92	49.6	2.98	48.7
5′	3.65	49.4	3.52	49.7	3.63	49.1
5″	3.44	—	3.29	—	3.44	—
6	—	176.0	—	179.8	—	176.6
7′	2.49	36.0	2.23	39.4	2.25	39.0
7″	2.43	—	2.16	—	2.15	—
8	—	178.8	—	183.5	—	182.8
9	—	142.7	—	144.9	—	143.2
10′	5.06	116.5	4.98	115.4	5.03	115.8
10″	4.78	—	4.74	—	4.75	—
11	1.76	25.0	1.77	25.1	1.78	25.0

Table 2. Homonuclear (^1H, ^1H) coupling constants in D_2O (Hz, error 0.3 Hz) used in the conformational analysis of kainic acid at different pH values

	^3J/Hz		
	pH 3	pH 7	pH 11
2, 3	<1	2.6	2.8
3, 7′	6.1	6.3	6.1
3, 7″	7.3	8.5	7.3
3, 4	5.9	6.0	6.1
4, 5′	8.0	7.4	6.6
4, 5″	11.3	11.2	9.5

The number indicates the predominant form in the pH zone considered (isoelectric zone **1**, neutral zone **2** and alkaline zone **3**).

groups. The coupling constants are calculated from 1-D spectra at 500 MHz and are confirmed by spectral simulation with the program 'NMR II' (Fig. 5). The prefixes *R* and *S* are used to unambiguously designate the configuration of prochiral centers. The 1-D experiments are not sufficient for the assignment of diastereotopic protons H(5) and H(7), this assignment is essentially obtained by analysing all the coupling constants values $^3J_{(H,H)}$ and $^3J_{(C,H)}$ from H(5), H(5″) and H(7), H(7″) (see below).

^1H–^1H Chemical shift correlation (COSY). The chemical shift of the H(2) (4.05 ppm) provides the starting point for tracing the coupling partners. A spin-coupling network is observed for the H(3), H(4), H(7), and H(5) protons, which provides unambiguous assignments of both 5-CH_2 and 7-CH_2 methylene groups.

^1H–^{13}C Chemical shift correlation (PFG-HMBC, pulse field gradient-heteronuclear multiple-bond correlation). From the assigned ^{13}C spectrum, it was possible to find a proton or a pair of protons bound to a carbon, using HMBC. The chemical shifts of each proton could then be determined by correlating the carbon–proton resonances.[34]

In order to confirm the interpretation of chemical shifts of the 5-CH_2 and 7-CH_2 methylene protons, an inverse heteronuclear correlation ^{13}C–^1H COSY experiment was carried out. Thus, it was possible to confirm the assignment of corresponding methylene protons, 5-CH_2 at higher frequencies (3.6 and 3.4 ppm) and 7-CH_2 at lower frequencies (2.25 and 2.15 ppm) as they are simultaneously coupled to the carbon C(5) at 49.1 ppm and C(7) at 39.0 ppm. The complete assignment of ^1H and ^{13}C signals was achieved at different pH values and was given in Tables 1 and 2, except for the individual diastereotopic methylene protons.

Assignment of the diastereotopic protons. The relative stereochemistry of kainoid amino acids have been analysed in detail by NMR chemical shifts[35] but the assignment of the individual diastereotopic methylene protons was particularly difficult. Sometimes, the homonuclear coupling constants and the NOE experiments are not sufficient to allow unambiguous assignments.[36,37] A simpler procedure is available as in addition to the α-proton, there are other nuclei that will be coupled over three bonds to the β-protons, namely the α-carbon (^{13}C). Then, it was necessary to define the $^3J_{(C,H)}$ coupling constants

Table 3. Heteronuclear (^{13}C, ^1H) coupling constants in D_2O (Hz, error 0.3 Hz). Torsion angles, calculated[a] coupling constants (^3J Hz) and NOEs allowing the determination of the position of the double bond

	NMR (^3J Hz)	Theoretical torsion angles/° (^3J Hz) Up	Down
4-H, 11-C		−146.6	40.5
	2.9	(4.9)	(3.3)
4-H, 10-C		33.8	−143.4
	4.8	(3.5)	(4.6)
	NOEs	**Inter-proton distances (Å)**	
4-H, 11-Me	[4-H] 11Me large	3.8	2.3
5*R*-H, 10″-H	[5″-H]10″H large	4.8	2.3

[a]The coupling constants values $^3J_{HH}$ and $^3J_{HC}$ were calculated by using Karplus type-equations: $^3J = A\cos^2\phi + B\cos\phi + C$ with different coefficients in the homonuclear case[40] ($^3J_{HH}$) A = 9.5, B = −1.3 and C = 1.6 and in the heteronuclear case[30] ($^3J_{HC}$) A = 5.7, B = −0.6 and C = 0.5.

Table 4. Homonuclear (^{1}H, ^{1}H) and heteronuclear (^{13}C, ^{1}H) coupling constants in D_2O (Hz, error 0.3 Hz) corresponding to the torsion angle χ_1 used in the conformational analysis of kainic acid and for the assignment of the diastereotopic methylene protons at C(5). Torsion angles and calculated[a] coupling constants (^3J Hz) computed for the 10 *envelopes* generated by molecular modelling[b]

	Theoretical torsion angles/° (^3J Hz)[a]											
Rotamer around χ_1 *envelopes*	**A 144.8** E_1	**B 73.4** E_2	**A 150.3** E_3[d]	**B 81.0** E_4	**B* 111.8** E_5	**B 88.1** ^1E	**A 163.6** ^2E	**B 76.4** ^3E	**A* 131.2** ^4E	**B* 122.0** ^5E	**NMR** ^3J Hz	**MD**[c]
2, 3	−98.5	−169.7	−90.1	−156.4	−130.1	−152.5	−74.8	−169.1	−101.5	−124.5		
	(2.0)	(12.0)	(1.6)	(10.7)	(6.4)	(10.1)	(1.9)	(12.0)	(2.2)	(5.3)	2.6	2.8
3, 4	1.98	27.3	−42.2	35.6	−31.2	−5.7	−27.6	35.6	44.6	22.4		
	(9.8)	(8.0)	(5.9)	(6.8)	(7.5)	(9.7)	(7.8)	(6.8)	(5.5)	(8.6)	6.0	5.8
4, 5′	89.0	4.9	32.6	−27.1	51.4	33.9	112.5	−16.7	48.0	80.4		
	(1.6)	(9.7)	(7.2)	(8.0)	(4.5)	(7.1)	(3.4)	(9.0)	(5.0)	(1.6)	7.4	5.0
4, 5″	−28.9	122.6	150.8	89.9	172.4	152.5	−5.6	100.8	168.8	−37.5		
	(7.6)	(5.1)	(10.0)	(1.6)	(12.2)	(10.3)	(9.7)	(2.2)	(12.0)	(6.5)	11.2	12.0
2-H, 4-C	142.6	81.4	155.3	94.9	117.3	97.5	161.8	81.4	143.6	116.3		
	(4.6)	(0.5)	(5.7)	(0.6)	(1.9)	(0.6)	(6.2)	(0.5)	(4.7)	(1.8)	4.0	4.3
2-H, 7-C	63.3	4.4	31.5	−34.4	53.5	45.5	56.5	54.9	21.3	56.2		
	(1.4)	(5.6)	(4.1)	(3.9)	(2.2)	(2.9)	(1.9)	(2.0)	(4.9)	(1.9)	4.7	4.5
4-H, 2-C	122.0	141.7	84.1	150.3	82.8	107.9	95.1	148.3	72.3	140.2		
	(2.4)	(4.5)	(0.5)	(5.3)	(0.5)	(1.2)	(0.6)	(5.1)	(0.8)	(4.3)	<1	0.8
5′-H, 2-C	−76.3	−131.8	−117.0	96.6	−162.8	−155.0	−89.4	−115.7	−142.9	−79.1		
	(0.7)	(3.4)	(1.9)	(0.6)	(6.2)	(5.7)	(0.5)	(1.8)	(4.6)	(0.6)	3.3	4.8
5′-H, 3-C	90.5	108.5	141.3	82.4	160.5	142.4	114.4	94.4	156.9	81.8		
	(0.5)	(1.2)	(4.4)	(0.5)	(6.1)	(4.5)	(1.7)	(0.6)	(5.9)	(0.5)	5.2	5.9
Assignment												
5′-H											*S*	
5″-H											*R*	

[a]The coupling constants values $^3J_{HH}$ and $^3J_{HC}$ were calculated by using Karplus type-equations: $^3J = A\cos^2\phi + B\cos\phi + C$ with different coefficients in the homonuclear case[40] ($^3J_{HH}$) A = 9.5, B = −1.3, and C = 1.6 and in the heteronuclear case[30] ($^3J_{HC}$) A = 5.7, B = −0.6, and C = 0.5.
[b]The E_1, ^2E, and ^5E have not been generated by the different MD protocols.
[c]The MD results lead to the averaging 10% Aa (^4E) +22% Ab (^4E) + 53% Ac (^4E) + 15% Ba ($^E5$) in solution. This correspond to 85% ^4E (major in the solution) +15% E_5. The $\Sigma\Delta J$ MD/NMR = 6.5. For each *i* the conformational microstate, the average coupling constant can be computed from the following:
$^3J(HH) = \Sigma Pi * {}^3J_i\,(HH)$
$^3J(HC) = \Sigma Pi * {}^3J_i\,(HC)$
$[J_{2,3} = 85\% * J_{2,3}\,(^4E) + 15\% * J_{2,3}\,(E_5) = 2.8\text{ Hz}\ (J_{obs} = 2.6)]$
[d]The E_3 conformation corresponds to the structure of KA obtained by X-ray diffraction.[46]

of both diastereotopic protons and use these values in conjunction with $^3J_{(H,H)}$ to define the conformation of the C(2)–C(3)–C(7)–C(8) fragment (Tables 3–5). One method for the quantitative determination of heteronuclear coupling constants usually fulfils these demands: the 2D $J\delta$ selective INEPT[38] using polarization transfer from ^{1}H to ^{13}C. The homonuclear and heteronuclear three-bond coupling constants, necessary for the assignments of the diastereotopic protons at C(5) and C(7) are listed in Tables 4 and 5, respectively.

The coupling constants measured from H(7′) and simultaneously H(7″) protons provide evidence for the identification of the major rotamer. From the large $^3J_{3,7''}$ and $^3J_{C(2)H(7')}$ values compared to the small ones $^3J_{3,7'}$ and $^3J_{C(2)H(7'')}$, we can deduce the position of the corresponding protons in the Newman projection. These values are in good agreement with the calculated coupling constants of the *gauche* g^--*c* χ_2 rotamer (Fig. 3). One can use the ^3J ^{13}C–^{1}H coupling constants for the diastereotopic proton attribution[36] as these ^{13}C–^{1}H coupling constants are 'out of phase' with the ^{1}H–^{1}H coupling constants. Hence in the '**c**' rotamer (Fig. 3), for example, H(7_S) and H(7_R) are *trans* and *gauche*, respectively to H(3), and H(7_S) and H(7_R) are *gauche* and *trans* to the carbon C(2). The experimental NMR data from H(7) measured at pH 7, $^3J_{3,7}$ (6.3 Hz), $^3J_{3,7''}$ (8.5 Hz), $^3J_{C(2)H(7')}$ (6 Hz), $^3J_{C(2)H(7'')}$ (3.7 Hz), $^3J_{C(4)H(7')}$ (3 Hz) and $^3J_{C(4)H(7'')}$ (3.7 Hz) allow us to assign H(7_R) to H(7′) and H(7_S) to H(7″).

The position of the H(5) relative to the face of the 5-membered ring is defined by the NOE experiments involving H(5″) as H(5″) and H(7″) [or H(7_S)] are located in the same face (Fig. 4). We can also deduce the axial or equatorial position of H(5″) from the spin system value of its neighbouring nucleus H(4). The large $^3J_{4,5''}$ value (11.2 Hz) shows that H(5″) and H(4) are *trans* diaxial (Fig. 2). The NOE [7″-H]5″-H and the $^3J_{4,5''}$ coupling constant allow us to assign H(5_R) to H(5″) and H(5_S) to H(5′).

2-D nuclear Overhauser enhancement experiments (NOE). A 2-D phase-sensitive ^{1}H NOESY experiment

Table 5. Homonuclear (^{1}H, ^{1}H) and Heteronuclear (^{13}C, ^{1}H) coupling constants in D_2O (Hz, error 0.3 Hz) corresponding to the torsion angle χ_2 used in the conformational analysis of kainic acid. Torsion angles, calculated[a] coupling constants (^3J Hz) and NOEs computed for KA for the second torsion angle (χ_2) relative to the major *envelope* ^{4}**E**

	^3JHz NMR	a	b	c	MD[b,c]
		Theoretical torsion angles/° (^3J Hz)[a]			
3, 7′		−173.6	52.2	−64.3	
	6.3	(12.3)	(4.4)	(2.8)	5.5
3, 7″		71.2	−54.8	−180.0	
	8.5	(2.2)	(4.0)	(12.4)	8.0
7′-H, 2-C		65.7	63.1	171.7	
	6.0	(1.2)	(1.4)	(6.7)	4.2
7′-H, 4-C		49.4	174.6	56.6	
	3.0	(2.6)	(6.7)	(1.9)	3.1
7″-H, 2-C		−49.5	−175.2	56.0	
	3.7	(2.5)	(6.7)	(1.9)	3.1
7″-H, 4-C		−164.6	64.6	−59.1	
	3.7	(6.3)	(1.3)	(1.7)	2.8
Assignment					
7′-H	*R*				
7″-H	*S*				
	NOEs	**Inter-proton distances (Å)**			
2-H, 7S-H	[2-H]7″-H large	2.5	3.7	2.7	
2-H, 7R-H	[2-H]7′-H medium	2.8	2.5	3.7	
SR-H, 7S-H	[5″-H]7″-H large	4.0	3.7	2.5	
SR-H, 7R-H	[5″-H]7′-H medium	2.5	4.0	3.5	

[a] The coupling constants values $^3J_{HH}$ and $^3J_{HC}$ were calculated by using Karplus type-equations: $^3J = A\cos^2\phi + B\cos\phi + C$ with different coefficients in the homonuclear case[40] ($^3J_{HH}$) A = 9.5, B = −1.3, and C = 1.6 and in the heteronuclear case[30] ($^3J_{HC}$) A = 5.7. B = −0.6, and C = 0.5.
[b] The MD results lead to the averaging 10% Aa (^{4}E) +22% Ab (^{4}E) +53% Ac (^{4}E) + 15% Ba (^{E}5) in solution. This corresponds to 25% a + 22% b + 53% c.
[c] R ΔJ MD/NMR = 4.7. For each *i* the conformational microstate, the average coupling constant can be computed from the following:
$^3J(HH) = \Sigma\ Pi * {}^3J_i\ (HH)$
$^3J(HC) = \Sigma\ Pi * {}^3J_i\ (HC)$
[$J_{3,7'}$ = 25% * $J_{3,7'}$ (a) + 22% * $J_{3,7'}$ (b) + 53% * $J_{3,7'}$ (c) = 5.5 Hz (J_{obs} = 6.3)].

in D_2O was performed using a time proportional phase-increment with τ_m = 500 ms.[39]

A spatial proximity between H(10) and Me(11) which reveals that H(10) and Me(11) are *cis*, that is, located in the same part of the double bond plane (Fig. 4). Moreover, the NOE [4-H]11-Me and especially the measured value (2.9 Hz) of the $^3J_{C(4)H(Me)}$ coupling constant (Table 3) allow us to conclude the 'down' stereochemistry of the double bond. This 'down' orientation is confirmed by the NOE [10′-H]5″-H (Table 4). In addition, this last connectivity allows us to confirm the *R* assignment of the H(5″) proton (Fig. 4).

It can be noted that the NOEs observed from H(7″), [2-H]7″-H and [5″-H]7″-H show the spatial proximities of the H(7″) proton with both H(2) and H(5″) (Fig. 4). In Table 5, the theoretical distances, evaluated from the three 'a, b, c' χ_2 rotamers can be compared to the NOEs obtained by NMR. All these observations may then be rationalized by the presence of a preferred 'c' χ_2 rotamer (Figs 3 and 4) and the diastereotopic assignment of the protons H(7′), H(5″) and H(7″), H(5′) as *R* and *S*, respectively.

Conformation around the χ_1 torsion angle. The $^3J_{^1H,^1H}$ coupling constants are helpful to determine the axial or equatorial position of the protons with respect to the five-membered ring, pyrrolidine. At the same time, the determination of long-range coupling constants $^3J_{^{13}C,^1H}$ provides important structural information, in particular about the orientation of the substituents (2-carboxyl and 4-isopropenyl groups) on the five-membered ring (Tables 3–5).

The presence of the two bulkier substituents leads to a predominant A* and/or A χ_1 [α-CO_2^-–C(2)–C(3)–C(7)] rotamer (130–170°) instead of the B or/and B* χ_1 one (70–120°): this is shown by the $^3J_{2,3}$ experimental value (2.6 Hz).

Indeed, the dihedral angle H(2)–C(2)–C(3)–H(3) of the A* (and/or A) conformations leads to a theoretical value $^3J_{2,3calc}$ = 2.2 Hz ($\phi_{2,3} \approx -101.9°$ for A*) or $^3J_{2,3calc}$ = 1.6 Hz ($\phi_{2,3} \approx -90.0°$ for A) in the corresponding *envelopes* (^{4}E, $\mathbf{E}_1$, ^{2}**E**, and $\mathbf{E}_3$). However the other B* (and/or B) conformations give $^3J_{2,3calc}$ = 5.3–6.4 Hz ($\phi_{2,3} \approx -125$–$130°$ for B*) or $^3J_{2,3calc}$ = 10.1–12.0 Hz ($\phi_{2,3} \approx -160°$ for B) in the corresponding *envelopes* ($\mathbf{E}_5$, ^{5}**E**, ^{1}**E**, $\mathbf{E}_2$, ^{3}**E**, and $\mathbf{E}_4$) (Table 4). All the theoretical angle values are deduced from the molecules generated by molecular modelling study. The comparison between calculated and experimental $^3J_{2,3}$ values allowed us to conclude that A* (and/or A) χ_1 [α–CO_2^-–C(2)–C(3)–C(7)] rotamer are the major ones in solution.

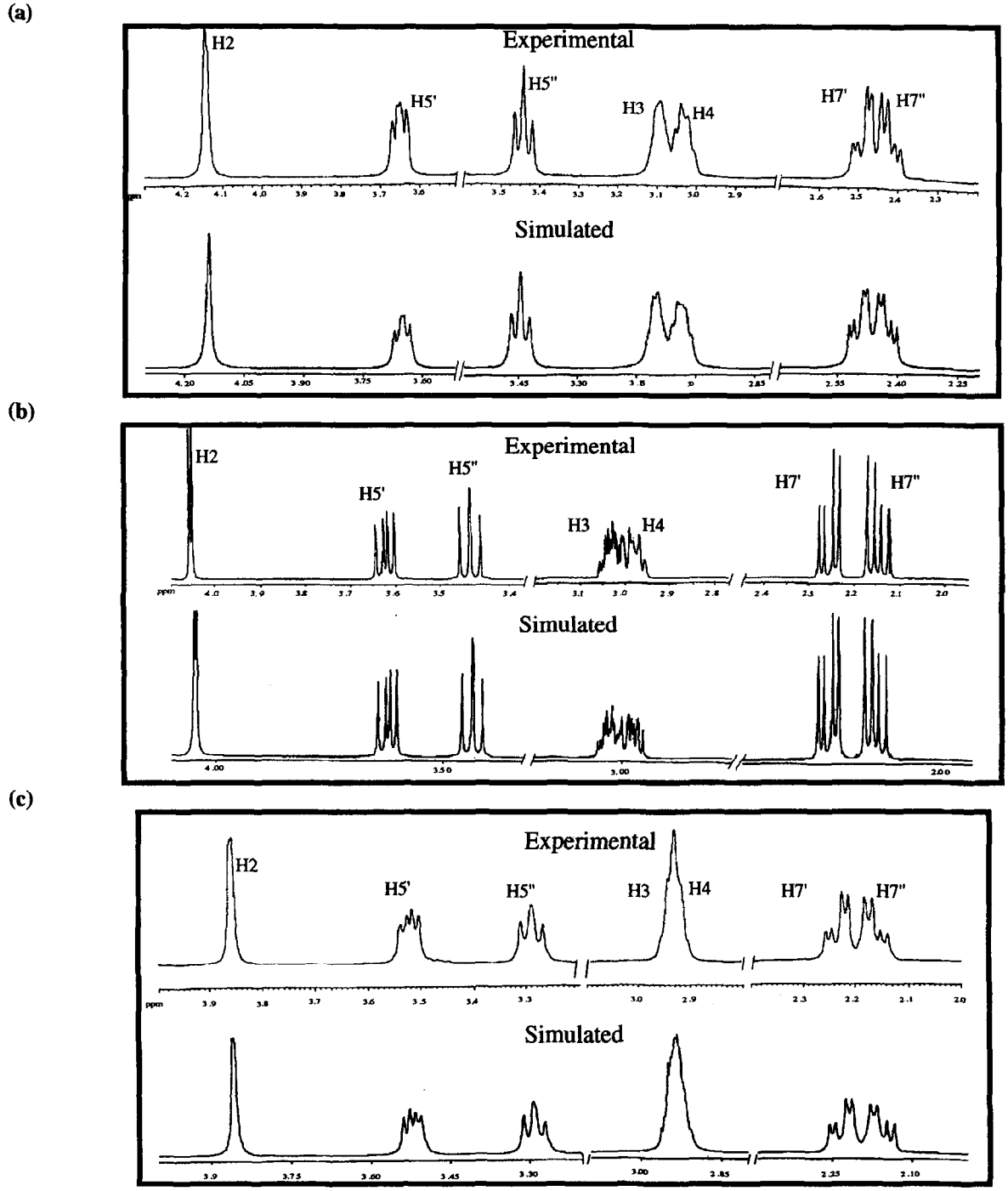

Figure 5. Details of the 500 MHz ^{1}H spectrum and simulation of the signals of KA (a) at isoelectric pH; (b) at neutral pH; and (c) at alkaline pH.

Our observed NMR values, $^3J_{2,3}$ = 2.6 Hz, $^3J_{C(4)H(2)}$ = 4.0 Hz, and $^3J_{C(7)H(2)}$ = 4.7 Hz (Table 4) should include an almost exclusive participation (≈ 90%) of A* (and/or A) χ_1 rotamers (120–170°) related to the *envelopes* (^{4}E, $\mathbf{E}_1$, $^2\mathbf{E}$, and $\mathbf{E}_3$) since both A* (and/or A) conformations are characterized by the calculated values, $^3J_{2,3}$ = 2.2 (1.6) Hz, $^3J_{C(4)H(2)}$ = 4.7 (5.7) Hz, and $^3J_{C(7)H(2)}$ = 4.9 (4.1) Hz. A difference of 0.5 Hz compared with the calculated values, although not really larger than the experimental error (0.2–0.3 Hz) may be interpreted as a slight contribution (≈ 10%) of the conformer B* (and/or B). These last B* (and/or B) χ_1 rotamers (70–120°) are related to the *envelopes* $\mathbf{E}_5$, $^5\mathbf{E}$ (^{1}E, $\mathbf{E}_2$, $^3\mathbf{E}$, and $\mathbf{E}_4$) and are represented by the calculated values $^3J_{2,3}$ = 5.3–6.4 (12.0) Hz, $^3J_{C(4)H(2)}$ = 1.9 (0.5) Hz, and $^3J_{C(7)H(2)}$ = 2.2 (2–5.6) Hz.

Conformation of the χ_2 torsion angle. For this second torsion angle, the difficulties of interpreting coupling constants in terms of specific conformations are

lessened because a wealth of information is available concerning the magnitude of coupling constants for specific rotamers about this single bond. The observed average coupling constant is given by an average over all conformational space, the coupling constant for each conformation being multiplied by the statistical weight of that conformation. It is generally established[37] that there exist three minimum energy conformations, or rotamers, in which the substituents on the two carbon atoms are 'staggered'. Thus it is assumed that the NMR spectrum of the molecule is the weighted average of the spectra of each of the three rotamers (Fig. 3). Considering the relationship between the H(3) proton and each of the two diastereotopic H(7) protons, it is apparent that the H(3) and H(7) protons are either *gauche* g^+-b, g^--c ($\pm$ 60°) or *trans* *t*-a (180°). The coupling constants corresponding to these two arrangements are denoted J_g and J_t, respectively. The rotamer populations can be obtained only if the following happen:

(1) The homonuclear and heteronuclear coupling constants relative to protons H(7′) and H(7″) can be measured (Table 5).

(2) The proton resonances (*R* and *S*) can be assigned individually to protons H(7′) and H(7″) (see above).

(3) Accurate values for J_g and J_t are available. The relationship between the magnitude of the coupling constants across three bonds (vicinal coupling constants) and the dihedral angle ϕ is obtained from the theoretical calculations of Karplus

$$^3J = A + B \cos \phi + C \cos^2 \phi$$

where A, B and C are coefficients that depend on substituent electronegativity and orientation.

Using information from a variety of conformationally rigid compounds with substituents similar to those encountered in amino acids, De Marco et al.[40] have proposed a set of values for the constants A, B and C giving, approximately J_g = 3.3 Hz, J_t = 12.4 Hz, for $^3J_{HH}$ (A = 9.5, B = −1.3, and C = 1.6). For the heteronuclear coupling constants, Hricovini have determined the values: A = 5.7, B = −0.6 and C = 0.5, then the theoretical coupling constants are approximately J_g = 1.8 Hz, J_t = 6.5 Hz.[30]

In what follows, we will calculate the theoretical values of the conformationally informative coupling constants from torsion angles computed by MD, using Karplus type-equations (Table 5).

The average coupling constant observed from the two individual H(7) and H(7″) protons will then be

$$J_{3,7'} = P_a J_t + P_b J_g + P_c J_g$$

$$J_{3,7''} = P_a J_g + P_b J_g + P_c J_t$$

where P_a, P_b and P_c are the fractional populations of the three rotamers (Fig. 3) so that

$$P_a + P_b + P_c = 1$$

Thus, the experimental coupling constants $^3J_{^1H\text{-}^1H}$ ($^3J_{3,7'}$ and $^3J_{3,7''}$) and $^3J_{^{13}C\text{-}^1H}$ (the two $^3J_{C(2)H(7)}$ and the two $^3J_{C(4)H(7)}$) presented in Table 5 allow us to determine with tolerable precision the mole fractions for each rotamer—P_a, P_b, and P_c—(it appears that rotamer populations accurate to $\pm$ 10% can still be obtained). We can calculate the χ_2 rotamer populations and we have obtained '**a**' (26%), '**b**' (22%), and '**c**' (52%). The *gauche* g^--c χ_2 rotamer is confirmed to be the major one in neutral solution. At pH 3 and 11, the solution conformations are analysed from homonuclear coupling constants and rotamer populations calculated as described above. Then, the major conformers *e*-A* (and/or *t*-A) and g^--c are found to be also predominant in the acidic or alkaline solution. The electrostatic interactions are reduced and the preferred conformations are the sterically favoured ones (Table 2). The percentage of the '**c**' rotamer remains important but the percentage of the '**a**' rotamer increases (31% a + 23% b + 46% c).

Considering the rotamer distribution relative to the dihedral angles χ_1 and χ_2 [α-CO_2^-–C(2)–C(3)–C(7)–γCO_2^-], the NMR study of KA has demonstrated that the major species in aqueous solution are *e*-A* and/or *t*-A about χ_1 and g^--c about χ_2 directing the double bond 'down' parallel to the carboxymethyl group (Fig. 4). Furthermore these data will be confirmed by the molecular modelling work.

The MD study will allow us to specify the *envelope* type (^{4}E) of the pyrrolidine group corresponding to *e*-A* or/and *t*-A conformations. A variety of possibilities enable the conformational populations of χ_2 rotamers to be assessed in NMR solution. Thus, it is very important to compare the NMR results with those obtained from molecular modelling (Tables 3–5) in order to characterize all the different conformations present in solution at different pH values.

Molecular modelling

The structures of the pyrrolidine unit of kainate obtained from the pseudo rotational circuit of the five-membered ring were built with the software Insight II using DISCOVER program from the Biosym package. In addition to the 10 *envelopes*, the three 'a, b, c' χ_2 conformations have to be considered, then only 30 conformers were studied as the 'down' position of the double bond was determinated by the NOESY experiments.

Molecular mechanics. To mimic the solvent effect, the relative permittivity was set to be distance-dependent, $\varepsilon = R_{ij}$ in the description of the Coulombic interaction.[41] The standard method

consists of adjusting the value of ε (from 1 to 78 in water) to simulate the effect of solvent on the coulombic interactions whilst avoiding an explicit inclusion of modeled water molecules. In a previous study, the relative permittivity was adjusted to a value ε = 5 corresponding to the interactions in aqueous solution.[42]

Using the Boltzmann distribution, the relative population of each conformer is given by the expression:

$$P_i = \exp(-E_i/kT)/\Sigma \exp(-E_i/\mathrm{kT})$$

With the different dielectric constant, only three conformations can be modelled and minimized for the χ_1 torsion angle, [B]→{^{3}**E**, **E**$_4$}, [B*]→{**E**$_5$} and [A*]→{^{4}**E**}. We calculated the relative population of each conformer, but this was not entirely consistent with the NMR results.

A second protocol can be used with explicit solvent molecules incorporated during the run. We constructed solvation boxes (12–12–12 Å) containing KA and several (48) water molecules using periodic boundary conditions. A cut-off function of 11 Å was applied for non-bonded interactions and the relative permittivity was set to ε = 1. With the protocol in the solvation boxes, four χ_1 conformations were obtained, represented by the corresponding *envelopes*: [B]→{^{1}**E**, **E**$_2$, ^{3}**E**, **E**$_4$}, [B*]→{**E**$_5$}, [A*]→{^{4}**E**} and [A]→{**E**$_3$}.

As the energies evaluated represent those of 'solute + $48H_2O$' systems, the corresponding energy of the minimized molecules is very difficult to calculate and then, their relative populations.

For this charged and flexible molecule, it is obvious that a MD study may have to be used to get a more reasonable stastistical participation of every structure. We have run experiments starting from the 30 theoretical *envelope* conformations to determine their frequencies in the interconversion. The results are summarized in Tables 3–5.

Molecular dynamics. The purpose of the MD method is to examine the structural and dynamic behaviour of the system. The MD algorithms are used to sample regions of conformational space that are not attainable using other computational procedures. The conformational searches are often performed at high temperatures as the large amount of kinetic energy present allows high potential energy barriers separating interesting regions of conformational space to be crossed.

Temperature factor. For a preliminary exploration of the conformational space, after energy minimization and an equilibration period of 4 ps, we perform a 50 ps MD run at 300 K with periodic temperature jumps to 600 K to supply the system with energy. The 50 ps trajectory is sampled every picosecond and the remaining structures are then minimized by molecular mechanics and stored; during this process, 1500 structures are generated. These results cannot lead to a statistical evaluation of the different conformations which participate in the NMR solution. At high temperature the molecule explores more states, however the fraction of time it spends near the lowest energy states is smaller.

Sampling time. To find an optimal protocol for better sampling and statistical evaluation, another factor has to be considered, the time of the MD run. This should be sufficient to sample all of the conformational space. The minor difference observed between multiple long MD runs (200 ps) and one very long MD run (2 ns) encouraged us to use a method of multiple starting points[43] in order to better sample phase space.

The stability of the different conformers was tested by a 200 ps dynamics protocol at 300 K. The statistical evaluation will be carried out during this process from 6000 generated structures. The experiments are first carried out with the value of the relative permittivity ε = 5, 78 and afterwards, the study was developed at neutral pH in a box filled with water molecules and the relative permittivity was set to ε = 1.

The coupling constants were calculated from the corresponding dihedral angles of each conformer generated by MD (Tables 3–5). Averaging is required to correctly predict the conformational properties like *J*-couplings. By using *Pi*, the fractional population for each *i*th conformational microstate, the average coupling constant can be computed from:

$$^3J_{(HH)} = \Sigma\, Pi * {}^3Ji_{(HH)} \quad \text{and} \quad {}^3J_{(HC)} = \Sigma\, Pi * {}^3Ji_{(HC)}$$

Experimental values were compared to the calculated values from the conformational equilibrium generated by the summed MD trajectories (Table 3–5). The different experiments were analysed and we found a good correlation (Fig. 6a, Tables 4, 5) between the NMR coupling constants, and those calculated from the conformational averaging obtained with the dielectric constant ε = 5

[10% A*a (^{4}E) + 22% A*b (^{4}E) + 53% A*c (^{4}E) + 15% B*a (E$_5$)]

The $\Sigma\, \Delta(J_{calc} - J_{exp})$ evaluated from about 15 coupling constants ($J_{H,H}$ and $J_{C,H}$) lead to an average value (<Δ> ± 0.7 Hz) which show without ambiguity that solution averaging is well described in good agreement with the NMR data.

From this MD experiment [10% A*a (^{4}E) + 22% A*b (^{4}E) + 53% A*c (^{4}E) + 15% B*a (E$_5$)], the rotamer populations are evaluated at

[A* = 85%→{^{4}**E**}, B* = 15%→{**E**$_5$}, a = 25%, b = 22%, and c = 53%]

and are compared to the NMR results (Fig. 6b):

[A* (and/or A) = 90%, B* (and/or B) = 10%, a = 26%, b = 22%, and c = 52%].

We can observe an excellent agreement between the experimental NMR and the theoretical MD results from the calculated and the experimental coupling constants (Fig. 6a) and also from the rotamer populations obtained from MD and NMR data (Fig. 6b).

A problem with the use of MD searching for ligand binding conformations, particularly if the ligands are ions or highly charged molecules, is not to neglect protonation sites which will induce particular conformations. Thus, we have extended this study to different pH values. At pH 3 and 11, the conformational averaging obtained by MD according to the NMR results

[30% A*a (^{4}E) + 18% A*b (^{4}E) + 45% A*c (^{4}E) + 7% B*a (E_5)].

correspond to the following rotamer populations

[A* = 93%→{^{4}**E**}, B* = 7%→{$\mathbf{E}_5$}, a = 37%, b = 18%, and c = 45%]

in agreement with the experimental NMR data

[A* (and/or A) = 90%, B* (and/or B) = 10%, a = 31%, b = 23%, and c = 46%].

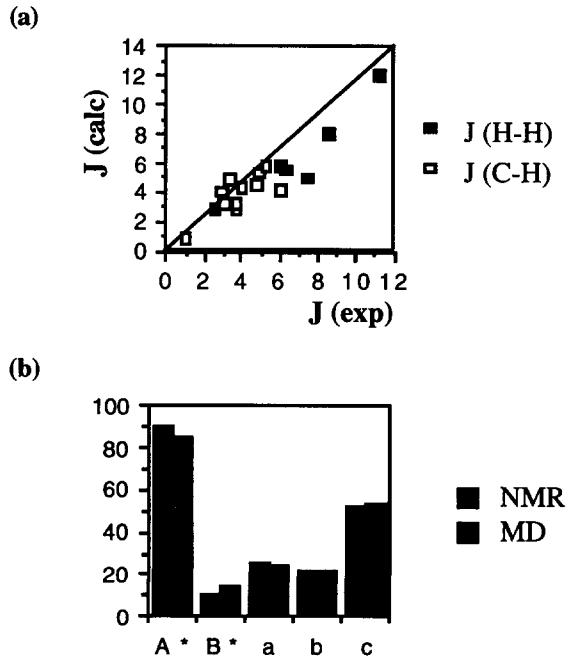

Figure 6. (a) Correlation between the experimental (NMR) and calculated (MD) coupling constant using the MD run which present the best correspondence (17 ^3J values) between MD and NMR data; and (b) between the observed (NMR) and calculated (MD) population of the rotamers.

At the different pH values, the fit between MD data and the experimental ones would also indicate that the conformational space was well sampled.[44,45] The small difference is attributed to a slight variation of the minor conformers that affects the conformational averaging in solution. Thus, all the structures achieved by MD will be taken into account for representing the compounds as every one can be in relation to the active site.

Similarity analysis

The NMR and MD studies of KA showed that the conformation *eg*$^-$-**A*c** embedded in the ^{4}**E** envelope is the major one in aqueous solution (Fig. 7a). The structure of KA was obtained by X-ray diffraction[46] and it can be shown that the resulting $\mathbf{E}_3$ envelope form was corresponding to the *tg*$^-$-**Ac** conformation. The following angles were found, respectively $\chi_1 = 160.4°$ and $\chi_2 = -76.9°$ and by comparison of NMR and X-ray structures it can be seen slight modifications (Fig. 7b).

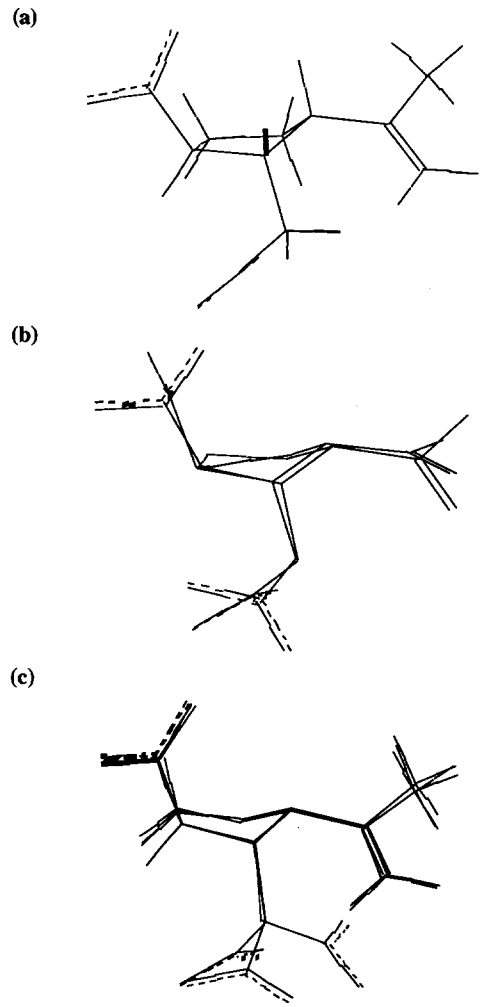

Figure 7. (a) Predominant *eg*$^-$**A*c** conformation embedded in the ^{4}**E** *envelope*, in aqueous solution; (b) Superimposition of the structure of KA obtained by X-ray diffraction with the major structure in aqueous solution; (c) Superimposition of the major A*c (^{4}E) conformation with all the other minor (^{4}E) *envelopes*: the A*a (^{4}E) and A*b (^{4}E).

The superimposition of C(1) and of the central atoms of the two functional groups, that is, the α-N and α-C(2) (α-CO) of the different conformers deduced from the NMR and MD data displays conformational similarities: we take around 90% of the solution into account, which are represented by the ^{4}**E** *envelope* conformation (Fig. 7c): **A*a** (^{4}E), **A*b** (^{4}E), **A*c** (^{4}E).

To argue about the conformation which binds to the receptor, we would like to refer the following compounds which do not have kainate skeleton such as γ-methyl-glutamate [(2*S*,4*R*)-4-methylglutamic acid][47] or **4E** and CPG-IV [2-(2-carboxy-4-methylenecyclopentyl)glycine].[22] Electrophysiological experiments in the new-born rat spinal motoneurons suggested that CPG-IV was a potent agonist of kainate receptors.[22] In this last compound, the rotation about C(3)–C(4) bond (χ_2 dihedral angle) being froozen, the nine conformations of glutamate or γ-methyl-glutamate are restricted to be only three rotamers resulting from the rotation about C(2)–C(3) bond (χ_1 dihedral angle) (Fig. 1a) .

CPG-IV is conformationally restricted glutamate analogue in which the cyclopentyl ring fixes partially the glutamate chain, about [C(3)–C(4)]. Concerning the rotamer around the α-amino acid moiety of CPG-IV, it can be assumed that C(2)–C(3) bond can rotate freely while rotation around the C(3)–C(4) bond is totally restricted by the five-membered ring and χ_2 [C(2)–C(3)–C(4)-γ-CO_2^-] torsion angle leads to forms characterized by an intermediate angle value between two *gauche* g^--c ($\chi_2 = -60°$) and g^+-b ($\chi_2 = 60°$) orientations.

Comparison with γ-methyl-glutamate (4E), a specific ionotropic KA agonist. One analogue with a methyl group at the four-position, the [(2*S*,4*R*)-4-methylglutamic acid] **4E** has been tested on the ionotropic KA receptor and it was identified as having exceptional selectivity for KA receptor subtype comparable to KA itself.[47]

The conformation of KA being totally elucidated and including a major one eg^--A*c and the minor ones (eg^+-A*b and *et*-A*a conformations), it was possible to make a suggestion about the structure-function relationship.

In view of the biological activity, we can compare these structural results to those obtained for the **4E** isomer. An identical set of conformations represented the **4E** solution,[48] the major conformation tg^--Ac and the same ensemble of minor conformers like tg^+-Ab and g^+t-Ba, which represent 20% of the **4E** solution. The g^+t-Ba conformation is sterically favoured for unprotonated molecule **4E** (pH 10) while at pH 3, this conformation is present in small amounts as the protonation of the distal acid induced a slight contribution of the conformation g^+g^--Bc in **4E** solution.

Figure 8 shows the superimposition of the eg^--**A*c** conformation of KA compound in qualitative agreement with the two types (tg^--Ac and g^+g^--Bc) of the potential active residues arrangement of **4E** isomer (RMS of deviation between heavy atoms ≤0.4 Å) since *e*-A* is intermediate between *t*-A and g^+-B rotamer. This illustrated the fact that the conformation at the receptor binding site might be relevant to one (or more) of these structures and the eg^--**A*c** (or/and tg^--Ac) conformation was observed to be specific to the ionotropic KA receptor.

Bound conformations to glutamate receptors. Glutamate activates two types of receptors, the ionotropic (NMDA, AMPA and KA) and the metabotropic (mGluRs) receptors.[13,49,50] Then it was interesting to include discussion on the specificity of contributor drug conformations concerning the different binding affinities at ionotropic and metabotropic receptors.

Since the *cis*-ACPD isomer, the (2*S*)-4-methyleneglutamic acid] and the (2*S*,3*S*,4*S*)-CCG (known as L-CCG-IV) were found to preferentially activate NMDA subtype receptors, our previous studies[48,51,52] have provided clear evidence that B*, B and c*, c conformations corresponded to the active rotamers of glutamates C(2)–C(3) and C(3)–C(4) bonds. Then, we concluded that the g^+g^--Bc (or B*c, Bc*) rotamer would be the most plausible conformation of glutamate required for binding to NMDA receptors in agreement with the pharmacophore suggested.[53]

The KA presents also a low activity to the metabotropic receptor and so it was interesting to compare the structural solution obtained for this compound to other compounds, known to activate the mGluRs receptors.

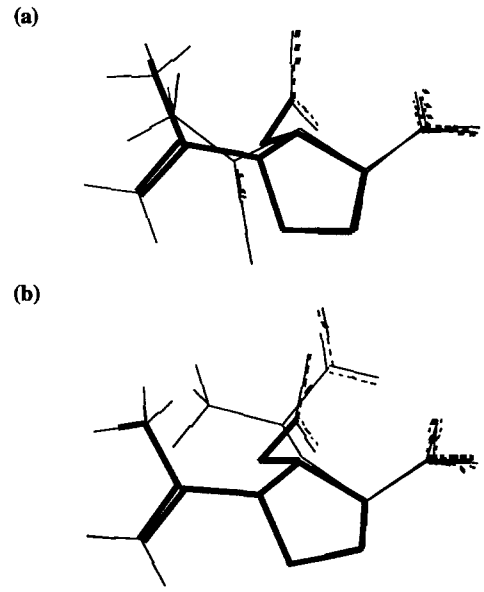

Figure 8. Superimposition of the eg^--**A*c** conformation of kainic acid compound with the two types (a) tg^--Ac and (b) g^+g^--Bc of the potential active residues arrangement of ^{4}**E** isomer.

The (1*S*,3*R*)-*trans*-ACPD analogue, potent agonist on the mGluRs receptor, adopts multiple conformations and it belongs to the conformational classes A, A*, B*, B and a, a*, b*, b conformations corresponded to the active rotamers of glutamates C(2)–C(3) and C(3)–C(4) bounds. Another analogue (2*S*,4*S*)-4-methylglutamic acid **4T** which was a potent agonist of mGluR1 has been studied and it was shown that it belongs mainly (60%) to the conformers tg^+-Ab (and also Ab*, A*b*). The *tt*-Aa and g^+t-Ba (and also g^+g^--Bb) conformations participate a little (10%) in the neutral **4T** solution.[48] Then, we concluded that the tg^+-Ab (or Ab*, A*b*) rotamer would be the most plausible conformation of glutamate required for binding to mGluR1 receptor. At last, the results obtained for the (2*S*,3*R*,4*S*)-CCG agonist analogue (known as L-CCG-I) which exhibited a mGluR2 activity[52] show that the conformation of glutamate *tt*-Aa or *tt*-Aa* regarding the carbon chain are important factors for the mGluR2 subtype receptor.

Since the conformational analysis of the KA shows that the solution structure is composed of 10% A*a + 22% A*b + 53% A*c + 15% B*a, we can conclude that its binding conformations of the KA and mGluR1 and mGluR2 receptors corresponds to the conformations A*c, A*b and A*a, respectively. The biological activity of glutamate analogues depends on many factors, and these may include their conformation in solution. This aspect makes restricted analogues interesting tools for studies of conformational preferences of glutamate subtype receptors. Thus, the binding conformations of the glutamatergic receptors corresponds to the conformation *t*-A, g^+-B and *t*-a, g^+-b, g^--c with a selectivity for the two receptors as ionotropic and metabotropic receptors. When the *t*-A, g^--c activate the KA receptors, the g^+-B, g^--c conformation activate the NMDA receptors and for the metabotropic receptor, the *t*-A, *t*-a and *t*-A, g^+-b conformations activate the mGluR2 and mGluR1 metabotropic receptors, respectively.

Conclusion

This study describes NMR and molecular modelling experiments designed to establish the likely conformation of free KA in dilute aqueous solution and in its possible ionized states. This key molecule is structurally similar to L-glutamate and has demonstrable selective agonist activity toward important neurotransmitter receptors. A discussion of the data from an earlier study[48] has been included in the present paper to enable a comparison between the various candidate ligand molecules since this information is important for further structure–activity studies targeted toward the design of superior compounds in this class.

KA contains an embedded L-glutamate moiety that is conformationally restricted about the 2,3-bond, so that the χ_1 torsion angle is essentially in the *e*-A* conformation, a structural feature that dramatically reduces the affinity for NMDA and metabotropic receptors, while increasing agonist activity at the KA receptor. It is important to note that KA retains a fair amount of conformational flexibility, not only with respect to the C(3) and C(4) appendages but also in the ring. Several *envelope* conformers (^{4}E, ^{1}**E**, ^{3}**E**, $\mathbf{E}_2$, $\mathbf{E}_3$, $\mathbf{E}_4$, and $\mathbf{E}_5$) are stable and these can differ quite substantially with respect to the relative positions of the substituent groups but one major form ^{4}**E** represents the low-energy conformer in aqueous solution, whatever the pH value is. The conformations relative to the carboxymethyl side-chain in the binding of KA derivatives have been discussed many times.[23,24,54] An NMR and molecular modelling study has resolved the preferred g^--*c* conformation of the C(3) carboxymethyl side-chain. The earlier observations suggested a favourable binding interaction due to either the resulting conformation of the carboxymethyl moiety or the orientation of the isopropenyl group. This study shows clearly the structural 'down' position of the double bond and this would be also associated with the KA activity.

The potencies of the KA interactions with the KA receptor should be at least partially dependent on the relative energies (and thus relative abundances) of each of KA conformations, and the C(3)-carboxymethyl and C(4)-isopropenyl groups may strongly influence these conformational preferences.

An important result of this study is the excellent agreement between the most significant conformer determined from the theoretical MD structures and the preponderant experimental NMR results in solution. Our study allows us to shed light on the complexity of this molecule and its conformation in solution is definitively elucidated. The NMR results combined with the molecular modelling showed that the predominant A* conformation [an almost exclusive participation (>90%)] adopts the ^{4}**E** envelope while the minor B* conformer [a slight contribution (<10%)] was found in the $\mathbf{E}_5$ envelope. These two methods allow us to calculate, for the second torsion angle (χ_2), the rotamer population: 'a, b and c'. The solution structure is composed by the major '**c**' rotamer (53%) and the minor ones a and b (approximately 22%, respectively).

Materials

NMR spectroscopy

NMR spectra were recorded on a Bruker AMX 500 spectrometer equipped with Silicon Graphics workstation. A sample of kainate (10 mg) was dissolved in 0.6 mL of D_2O to give a final concentration 0.08 mol dm^{-3} for the different isomers. The pH (in fact pD = pH −0.4, uncorrected here) was adjusted by addition of DCl or NaOD. At pH 7 the sample was dissolved in an aq. NaD_2PO_4–Na_2DPO_4 buffer, and it was possible to attain concentrations of 0.08 mol dm^{-3} for ^{1}H and ^{13}C experiments.

The errors on the chemical shifts are 0.01 and 0.1 ppm for ^{1}H and ^{13}C, respectively. A crystal of 3-(trimethylsilyl)[2,2,3,3-$^2H_4$] propionic acid, sodium salt [$^2H_4$]TSP

was used as internal reference for the proton shifts, and for the carbon a value of the absolute frequency was used. The coupling constants are given with a precision of 0.3 Hz. The spectrum simulation was done on a Macintosh II computer using the software NMR II.

The Selective Inept (INAPT)[55] recorded with 32 K data points with a selective excitation of the H(2) proton allows us to differentiate the two carboxy groups [C(6) and C(8)].

The ^{1}H detected ^{1}H, ^{13}C-HMBC spectrum (PFG-HMBC, pulse field gradient heteronuclear multiple-bond correlation)[34] was recorded at 300 K with 16 scans, 256 experiments of 1024 data points, a sweep width of 4000 Hz in f_2 and 27,507 Hz in f_1. One millisecond half-sinusoid gradients of 28, 28, and 14 G/cm were used to select for protons attached to carbon and the delay of 80 ms which was optimum for two- or three-bond couplings.

The 2-D phase-sensitive ^{1}H NOESY experiment was performed in D_2O solution with τ_m = 0.5 s and the relaxation delay of 3.0 s.[39] FIDs were acquired (256 scans) over 3086 Hz into a 2 K data block for 256 incremental values of the evolution time.

The 2-D J δ selective INEPT[38] using the polarisation transfer from ^{1}H to ^{13}C gave long-range heteronuclear coupling constants ^3J (^{13}C–^{1}H). The selective excitation of a proton signal allows detection of a single doublet for the corresponding coupled carbon(s). At 500 MHz, selectivity was achieved by a DANTE-type pulse train generated by the decoupler channel. This experiment also allows us to analyse the 'a, b, c' rotamer populations. This experiment was recorded at 300 K with 256 scans of 4000 data points, 64 experiments, a spectral width of 220 ppm in f_2 and 62.5 Hz in f_1.

Computer simulations

The conformations of KA that were incorporated into the analysis were obtained using the BIOSYM molecular modelling software on a Silicon Graphics workstation.[56] Initial structures were built using the INSIGHT II builder module, which directly produced a coarse 3-D starting structures. To mimic ionization at neutral pH, an sp^{3+} hybridization was assigned to the amine of the main alkyl chain, increasing the molecular electrostatic total charge by +1.

To mimic the solvent effect, the relative permittivity was set to be distance dependent in the description of the coulombic interaction, $\varepsilon = R_{ij}$ ($\varepsilon = 5$).[42] A second protocol can be used with explicit solvent molecules incorporated during the run. We constructed solvation boxes containing KA and several water molecules using periodic boundary conditions. A cut-off function of 11 Å was applied for non-bonded interactions. The relative permittivity was set to $\varepsilon = 1$ and a box contained 48 (12–12–12) water molecules. The energies obtained are those of molecule + 48 H_2O systems.

Energy minimization and MD simulations were performed with the INSIGHT II Discover module, using the consistent valence force field (CVFF).[56]

The first step in the modelling consisted of minimizing the structure previously constructed, to find a local energy minimum on the potential energy hypersurface of the molecule. Calculations were performed according to several algorithms commonly used in molecular mechanics for choosing descent directions, namely steepest descent and conjugate gradient methods.

The second step of the conformational sampling procedure consisted of recording MD trajectories. Molecular conformers were sampled during a 200 ps MD trajectory at 300 K. A time step of 1 fs was used, and the system was equilibrated for 6 ps. A conformation was stored each 1 ps so that 200 conformations were recorded by the end of the MD simulation. For a preliminary exploration of the conformational space, after energy minimization and an equilibration period of 6 ps, we performed a 50 ps MD run at 300 K with periodic temperature jumps to 600 K to supply the system with energy (to pass conformational barriers). The 50 ps trajectory is sampled every ps and the remaining structures are then minimized by molecular mechanics and stored. The final conformers found with lowest energies were then further minimized to a gradient less than 0.01 kcal mol^{-1} to obtain their energies at higher accuracy.

The sampling every picosecond was supposed sufficiently large for a significant moving of the atoms and sufficiently short for a correct sampling of the conformational space. For an isolated molecule, the experiment takes about 15–30 min. For experiments in which the molecules are introduced into the solvation boxes, the CPU times are much longer (i.e. 24 or 48 h according to the protocol).

All molecular conformations were compared using the Analysis module of INSIGHT II. Conformational similarities were evaluated by calculating the RMS deviation between heavy atoms for each possible pair of the different structures. The results represent a group of stuctures whose small RMS deviations (<0.5 Å) suggested that they may belong to the same conformational family. Conformational representatives extracted from each family were compared for each compound, as well as between different ligands, using a superimposition procedure.

Acknowledgements

We thank J. Hart-Davis for skilful assistance.

References

1. Monoghan, D. T.; Bridges, R. J.; Cotman, C. W. *Annu. Rev. Pharmacol. Toxicol.* **1989**, *29*, 365.

2. Watkins, J. C.; Krogsgaard-Larsen, P.; Honoré, T. *Trends Pharmacol. Sci.* **1990**, *11*, 25.

3. Olney, J. W. *Annu. Rev. Pharmacol. Toxicol.* **1990**, *30*, 47.

4. Choi, D. W. *Neuron* **1988**, *1*, 623.

5. Meldrum, B. *Brain Res. Rev.* **1993**, *18*, 293.

6. Olney, J. W. *Neurobiol. Aging* **1994**, *15*, 259.

7. Choi, D. W.; Rothman, S. M. *Ann. Rev. Neurosci.* **1990**, *13*, 171.

8. Meguro, H.; Mori, H.; Araki, K.; Kushiya, E.; Kutsuwada, T.; Yamazaki, M.; Kumanishi, T.; Arakawa, M.; Sakimura, K.; Mishina, M. *Nature (London)* **1992**, *357*, 70.

9. Seegurg, P. H. *Trends Pharmacol.* **1993**, *14*, 297.

10. Palmer, E.; Monoghan, D. T.; Cotman, C. W. *Eur. J. Pharmacol.* **1989**, *166*, 585.

11. Tanabe, Y.; Masu, M.; Ishii, T.; Shigamoto, R.; Nakanishi, S. *Neuron* **1992**, *8*, 169.

12. Hayashi, Y.; Momiyama, A.; Takahashi, T.; Ohishi, H.; Ogawa-Meguro, R.; Shigemoto, R.; Mizuno, N.; Nakanishi, S. *Nature (London)* **1993**, *366*, 687.

13. Nakanishi, S. *Science* **1992**, *258*, 597.

14. McGeer, E. G.; Olney, J. W.; McGeer, P. L.McGeer, E. G.; Olney, J. W.; McGeer, P. L. *Kainic Acid as Tool in Neurobiology;* Raven: New York, 1978.

15. Ishida, M.; Shinozaki, H. *Br. J. Pharmacol.* **1991**, *104*, 873.

16. Ishida, M.; Shinozaki, H. *Brain Research* **1988**, *474*, 386.

17. Horikawa, M.; Hashimoto, K.; Shirahama, H. *Tetrahedron Lett.* **1993**, *34*, 331.

18. Konno, K.; Hashimoto, K.; Ohfune, Y.; Shirahama, H.; Matsumoto, T. *J. Am. Chem. Soc.* **1988**, *110*, 4807.

19. Kwak, S.; Aizawa, H.; Ishida, M.; Shinozaki, H. *Exp. Neurology* **1992**, *116*, 145.

20. Cantrell, B. E.; Zimmerman, D. M.; Monn, J. A.; Kamboj, R. K.; Hoo, K. H.; Tizzano, J. P.; Pullar, I. A.; Farrell, L. N.; Bleakman, D. *J. Med. Chem* **1996**, *39*, 3617.

21. Bridges, R. J.; Lovering, F. E.; Humphrey, J. M.; Stanley, M. S.; Blakely, T. N.; Cristofaro, M. F.; Chamberlin, A. R. *Bioorg. Med. Chem.* **1993**, *3*, 115.

22. Shimamoto, K.; Shigeri, Y.; Nakajima, T.; Yumoto, N.; Yoshikawa, S.; Ohfune, Y. *Bioorg. Med. Chem. Lett.* **1996**, *6*, 2381.

23. Horikawa, M.; Shima, Y.; Hashimoto, K.; Shirahama, H. *Heterocycles* **1995**, *40*, 1009.

24. Konno, K.; Hashimoto, K.; Shirahama, H. *Heterocycles* **1992**, *33*, 303.

25. Hashimoto, K.; Shirahama, H. *Syntheses of Neuroexcitatory Kainoids*, 1, R. T. T. India, 1991

26. Hashimoto, K.; Horikawa, M.; Shirahama, H. *Tetrahedron Lett.* **1990**, *31*, 7047.

27. Shimamoto, K.; Ohfune, Y. *J. Med. Chem.* **1996**, *39*, 407.

28. Altona, C.; Sundaralingam, M. *J. Am. Chem. Soc.* **1973**, *95*, 2333.

29. Haasnoot, C. A. G.; De Leeuw, F. A. A. M.; Altona, C. *Tetrahedron* **1980**, *36*, 2783.

30. Tvaroska, I.; Hricovini, M.; Petrakova, E. *Carbohydr. Res.* **1989**, *189*, 359.

31. Bendall, M. R.; Pegg, D. T. *J. Magn. Reson.* **1983**, *53*, 272.

32. Rutar, J. A. *J. Magn. Reson.* **1984**, *59*, 306.

33. Wong, T. C.; Rutar, V. *J. Am. Chem. Soc.* **1984**, *106*, 7380.

34. Hurd, R. E.; John, B. K. *J. Magn. Reson.* **1991**, *91*, 648.

35. Hashimoto, K.; Konno, K.; Shirahama, H. *J. Org. Chem.* **1996**, *61*, 4685.

36. Roberts, G. C. K.; Jardetzky, O. *Adv. Protein Chem.* **1970**, *24*, 447.

37. Jardetzky, O.; Roberts, G. C. *NMR in molecular biology*; Academic: New York, 1981.

38. Ladam, P.; Gharbi-Benarous, J.; Pioto, M.; Delaforge, M.; Girault, J. P. *Magn. Reson. Chem.* **1994**, *32*, 1.

39. Delsuc, M. A. Ph.D. thesis, Orsay, 1985.

40. De Marco, A.; Llinas, M.; Wüthrich, K. *Biopolymers* **1978**, *17*, 637.

41. Burt, S. K.; Mackay, D.; Nagler, A. T. *Computer-Aided Drug Design*; Perun, T. J.; Propst, C. L. Eds.; New York, 1989

42. Morelle, N.; Gharbi-Benarous, J.; Acher, F.; Valle, G.; Crisma, M.; Toniolo, C.; Azerad, R.; Girault, J. P. *J. Chem. Soc., Perkin Trans. 2* **1993**, 525.

43. Weiner, S. J.; Kollmann, P. A.; Case, D. C.; Singh, U. C.; Ghio, C.; Alagona, G.; Profeta, S.; Weiner, P. *J. Am. Chem. Soc.* **1984**, *106*, 765.

44. Kessler, C.; Griesinger, C.; Lautz, J.; Müller, A.; van Gunsteren, W. F.; Berendsen, H. J. C. *J. Am. Chem. Soc.* **1988**, *110*, 3393.

45. Hünenberger, P. H.; Mark, A. E.; van Gunsteren, W. F. *J. Mol. Biol.* **1995**, *252*, 492.

46. Nitta, I.; Watase, H.; Tomiie, Y. *Nature (London)* **1958**, *181*, 761.

47. Gu, Z. Q.; Hesson, D.; Pelletier, J. C.; Meccecchini, M. L. *J. Med. Chem.* **1995**, *38*, 2518.

48. Todeschi, N.; Gharbi-Benarous, J.; Acher, F.; Larue, V.; Pin, J. P.; Bockaert, J.; Azerad, R.; Girault, J. P. *Bioorg. Med. Chem.* **1997**, *5*, 335.

49. Hollmann, M.; Heinemann, S. *Ann. Rev. Neurosci.* **1994**, *17*, 31.

50. Pin, J. P.; Bockaert, J. *Curr. Opin. Neurobiol.* **1995**, 342.

51. Larue, V.; Gharbi-Benarous, J.; Acher, F.; Valle, G.; Crisma, M.; Toniolo, C.; Azerad, R.; Girault, J. P. *J. Chem. Soc., Perkin Trans. 2* **1995**, 1111.

52. Evrard-Todeschi, N.; Gharbi-Benarous, J.; Cossé-Barbi, A.; Thirot, G.; Girault, J. P. *J. Chem. Soc. Perkin Trans. 2*, accepted.

53. Ortwine, D. F.; Malone, T. C.; Bigge, C. F.; Drummond, J. T.; Humblet, C.; Johnson, G.; Pinter, G. W. *J. Med. Chem.* **1992**, *35*, 1345.

54. Ohfune, Y.; Shimamoto, K.; Ishida, M.; Shinozaki, H. *Bioorg. Med. Chem. Lett.* **1993**, *3*, 15.

55. Bax, A. *J. Magn. Reson.* **1984**, *57*, 314.

56. Dauber-Osguthorpe, P.; Roberts, V. A.; Osguthorpe, D. J.; Wolff, J.; Genest, M.; Hagler, A. T. *Proteins: Structure, Function and Genetics.* **1988**, *4*, 31.

(*Received in U.S.A.* 17 *February* 1997; *accepted* 12 *June* 1997)